Improved Whale Optimization Algorithm for Dynamic Optimal Power Flow with Renewable Energy Penetration

Kukuh Widarsono
Department of Electrical Engineering Institut Teknologi Sepuluh Nopember Surabaya, Indonesia | Department of Electrical Industrial Engineering, Politeknik Negeri Madura Sampang, Indonesia
7022211003@student.its.ac.id

Adi Soeprijanto
Department of Electrical Engineering, Institut Teknologi Sepuluh Nopember Surabaya, Indonesia
adisup@ee.its.ac.id (corresponding author)

Rony Seto Wibowo
Department of Electrical Engineering, Institut Teknologi Sepuluh Nopember Surabaya, Indonesia
ronyseto@ee.its.ac.id

Received: 20 November 2024 | Revised: 24 December 2024 | Accepted: 29 December 2024

 DOI: https://doi.org/10.48084/etasr.9662

ABSTRACT

This paper proposes the Improved Whale Optimization Algorithm (IWOA) method to solve the Dynamic Optimal Power Flow (DOPF) problem in Renewable Energy Systems (RES), taking into account the influence of Energy Storage (ES). The convergence performance of the Whale Optimization Algorithm (WOA) algorithm is enhanced by incorporating Fuzzy Logic Control (FLC) in the exploration phase. The FLC assists the IWOA agents in finding the optimal weight values more quickly. The weights generated by the IWOA method are dynamic, continuously adjusting based on the deviation or error in the agents' movement during each iteration, which is essential for locating the global optimum. This paper primarily uses FLC to determine the weights, accelerating the IWOA optimization process. The effectiveness of this method is tested on the IEEE 30-bus system with the integration of PV and ES. The findings of this study demonstrate the superiority of the IWOA method over the WOA algorithm, resulting in a lower generation cost of $25/day and a faster convergence time.

Keywords-Dynamic Optimal Power Flow (DOPF); Improved Whale Optimization Algorithm (IWOA); weight; Fuzzy Logic Control (FLC); Energy Storage (ES)

I. INTRODUCTION

Optimal Power Flow (OPF) is a critical component of the operation of the electric power system. OPF is the process of balancing the generation of power against the requirements of the load, taking into account the operational limitations of the generator. The objective of the OPF is to achieve a more efficient power flow model that aligns with economic, technical, and environmental imperatives [1]. The integration of renewable energy sources into the grid has been shown to introduce a significant degree of complexity to the OPF [2]. DOPF represents an advanced level of the OPF, emphasizing the operating relationship from the 1st to the 2nd hour and so on until 24 hours. However, DOPF reveals more fundamental challenges in the generator operating system. A multitude of methods and approaches have been employed to address power flow optimization problems, using mathematics [3-9]. However, the efficacy of these mathematical-based approaches is limited due to their reliance on a linear model to address the underlying dynamics. Consequently, Artificial Intelligence (AI) methods have gained popularity in conjunction with traditional mathematical approaches for addressing OPF problems [10-16]. The efficacy of various techniques, including the Sun Flower Optimization (SFO) algorithm, evolutionary algorithm-based adaptive robust optimization, FLC, Particle Swarm Optimization (PSO), and Gray Wolf Optimization (GWO), in addressing power flow optimization challenges has been validated. However, it should be noted that many meta-heuristic methods have limitations, including the tendency to become trapped in local optima and the often-lengthy computation times required. The issue of global warming has prompted researchers to study the potential of renewable energy as a source of electrical energy. Consequently, the integration of renewable energy in OPF has become pervasive.

Moreover, the implementation of renewable energy sources is being driven by a combination of policy incentives and heightened community awareness regarding the climate change and resource depletion, which periodically necessitates the integration of renewable energy sources [17]. Renewable energy offers a sustainable and low-emission alternative and has the potential to reshape the energy landscape, significantly reducing the environmental footprint of power generation [18-19].

The WOA, inspired by the hunting behavior of whales, is a meta-heuristic algorithm introduced in [20] that has been widely used for various optimization problems across various fields. However, the standard WOA has been the subject of criticism due to its limited accuracy, slow convergence rate, and challenges in avoiding local optima. To address these limitations, researchers have proposed several enhancements [21-23]. These enhancements include the following: an improvement in the performance of WOA using inertia weights [21], an enhancement in the use of adaptive weights and crossover strategies to improve solution quality and accelerate convergence [22], and an approach based on the nonlinear adaptive weight and golden sine operator [23]. This study proposes a novel approach for solving the DOPF problem using the IWOA. The efficacy of the WOA is augmented by the incorporation of a dynamic weight parameter into the movement of the whale agents. The determination of this parameter is achieved through the implementation of an FLC, which is configured with two inputs: error and delta error. The error is calculated based on the whale's current movement, while the delta error represents the difference between the current error and the previous error. This dynamic weight is updated at each iteration based on the values of the error and delta error, enabling the algorithm to improve both the convergence speed and solution optimality compared to the standard WOA. The IWOA is applied to solve the DOPF problem, which becomes increasingly complex when incorporating renewable energy sources, such as Photovoltaic (PV) systems. Addressing the challenges posed by the variability and intermittent nature of renewable energy sources, the integration of battery storage within the system serves to enhance its stability and feasibility.

II. PROBLEM FORMULATION

In this study, the IWOA method is proposed as a solution to the problems in DOPF. The stages for solving the problem will include:

A. Objective Function

The DOPF problem is defined by the following objective functions (1) and cost function (2), as expressed in:

$$min\ F_G = min\ \sum_{t=1}^{T}\sum_{i=1}^{N_G} C_{G,i} \cdot P_{G,i} \quad (1)$$

$$C_{G,i} = \sum_{i=1}^{N}(\alpha_i + \beta_i P_{Gi} + \gamma_i P_{Gi}^2) \quad (2)$$

B. Power Flow Formulation

The following equations are presented for the nonlinear power flow model:

$$P_i = \sum_{t=1}^{T}\sum_{j=1}^{N_B}|V_i| \cdot |V_j| \cdot |Y_{ij}|\, cos(\theta_{ij} - \delta_i + \delta_j) \quad (3)$$

$$Q_i = -\sum_{t=1}^{T}\sum_{j=1}^{N_B}|V_i| \cdot |V_j| \cdot |Y_{ij}|\, sin(\theta_{ij} - \delta_i + \delta_j) \quad (4)$$

$$P_{G,i}^{min} \le P_{G,i} \le P_{G,i}^{max} \quad (5)$$

$$Q_{G,i}^{min} \le Q_{G,i} \le Q_{G,i}^{max} \quad (6)$$

$$-S_{ij}^{max} \le S_{ij} \le S_{ij}^{max} \quad (7)$$

$$V_i^{min} \le V_i \le V_i^{max} \quad (8)$$

$$\theta_i^{min} \le \theta_i \le \theta_i^{max} \quad (9)$$

$$R_i^{down} \le P_{G,i}^{t+1} - P_{G,i}^{t} \le R_i^{up} \quad (10)$$

$$-P_{ES,ch}^{max} \le P_{ES} \le P_{ES,dis}^{max} \quad (11)$$

$$E_{ES,max} \le E_0 - \sum_{t=1}^{T} E_{ES,t} \le E_{ES,min} \quad (12)$$

Equations (3) and (4) express active and reactive power in bus i, respectively. Equations (5)-(9) express the maximum and minimum limits for the active and reactive power generation, transmission line capacity, voltage magnitude, and voltage angle, respectively. The generation ramping rates are constrained in (10). The charging and discharging rate of ES is constrained by the limit expressed in (11), while (12) imposes a limitation on the total energy stored in each period.

C. Energy Storage

In this paper, the operational limitations of the battery are examined. The objective of this research is to ensure that the battery operation is maintained in accordance with its capabilities, life, and energy availability for the subsequent period. The limitations of the battery are:

$$SOC_{min} < SOC < SOC_{max} \quad (13)$$

$$07.00\ \text{a.m} \le \text{Charging} \le 05.00\ \text{p.m} \quad (14)$$

$$06.00\ \text{p.m} \le \text{Discharging} \le 03.00\ \text{a.m} \quad (15)$$

$$P_{CH} \ge -8\ \text{MW}\ \&\ P_{DCH} \le 8\text{MW} \quad (16)$$

Equation (13) demonstrates the ES capacity. The process of charging the battery during the day and discharging at night is presented in (14) and (15), while variables P_{CH} and P_{DCH} denote the power required for charging and discharging the battery, respectively.

D. Photovoltaic Systems

PV systems are engineered to convert solar energy into electrical power. The electrical output of a PV system is influenced by the ambient temperature of the surrounding environment and the intensity of solar radiation. The subsequent calculation has been formulated to address this phenomenon:

$$P_{PV}(E_M) = P_{STC} \times \frac{n \times E_M}{E_{STC}}[1 + k(T_M - T_{STC})] \quad (17)$$

where P_{PV} is the actual power output of the PV system., P_{STC} is the maximum power output of the PV module, E_M is the incoming irradiance onto the PV modules, E_{STC} is the irradiance level, typically 1000 W/m^2, k is the coefficient accounting for the impact of temperature on the power output, as specified in the PV module's datasheet, T_M stands for the temperature of the PV module, T_{STC} is the reference temperature, and n is the total number of the PV modules used in the system.

III. WHALE OPTIMIZATION ALGORITHM

The WOA draws inspiration from the hunting behavior of humpback whales in the pursuit and capture of their prey. The movement of humpback whales during this process can be modeled in three primary phases: circling the prey, the exploitation phase, which includes both circular and spiral methods, and the exploration phase. A detailed mathematical model of the WOA has been presented in [20].

IV. PROPOSED METHOD (IMPROVED WHALE OPTIMIZATION ALGORITHM)

As shown in Figure 1, the novel method in IWOA employing FLC is presented. The introduction should provide a concise contextual overview of the work.

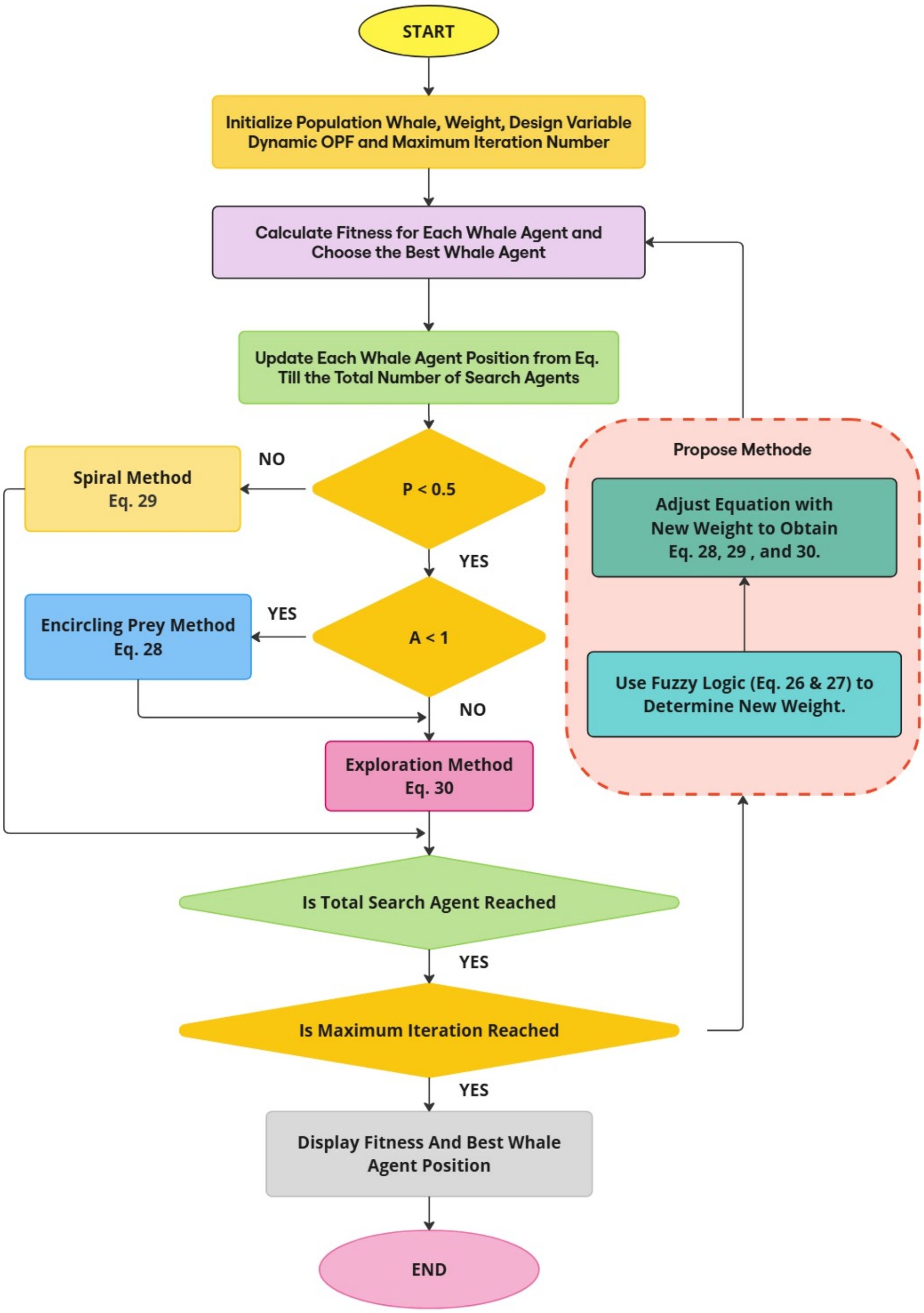

Fig. 1. IWOA flowchart.

The novel proposal at IWOA entails the incorporation of weight (w). The weights will be generated from the FLC, which is equipped with two inputs: error (E_t) and delta error (*DelE*). The error is derived from the movement of the whale, while the delta error is calculated as the difference between the current error and the previous one. Errors can be obtained from the whale movements during the exploration and exploitation stages in the WOA. The proposed scheme of the FLC for the weight generation is outlined in Figure 2.

Each FLC input is characterized by five membership functions: very close (vc), quite close (qc), close (c), quite far (qf), and far (f). The width of each input value is adjusted according to the power generation limits of each generator. The input errors are constrained to share the same width across their respective membership functions, whereas the delta errors are designed to deviate slightly, with a denser distribution valued at 0-50 (10% of the width value). This approach is intended to expedite the convergence of the whale to its target point. The membership functions for the error and delta error are presented in Figures 3 and 4, respectively, while the surface rules are shown in Figure 5.

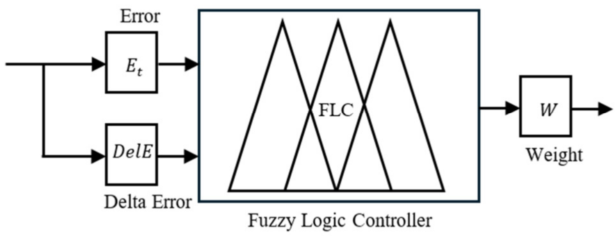

Fig. 2. FLC scheme for weight generating.

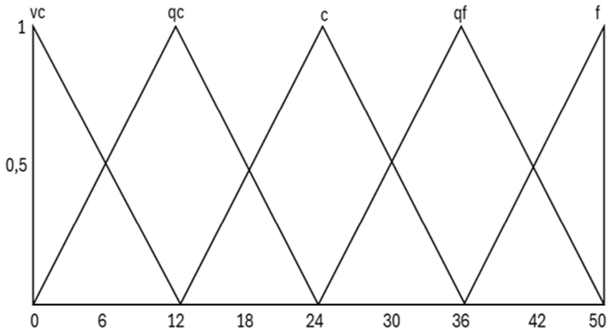

Fig. 3. Membership function of error.

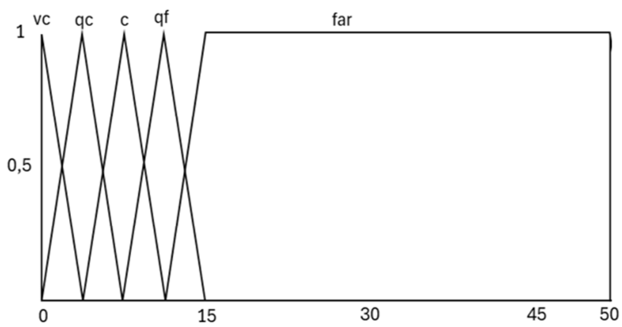

Fig. 4. Membership function of delta error.

The weights resulting from the FLC will be multiplied by (18) and (19). The ensuing details provide a comprehensive exposition on weight generation and its implementation in IWOA:

$$E_t = \vec{D} = |\vec{C}.\vec{X}^*(t) - \vec{X}(t)| \quad (18)$$

$$DelE = abs\,|E_{(t)} - E_{(t+1)}| \quad (19)$$

where E_t is the current error, $E_{(t+1)}$ is the previous error, and *DelE* is the delta error. Subsequent to the acquisition of the weight values from the FLC, the primary equation of WOA can be modified as:

$$\vec{X}(t+1) = \vec{X}^*(t) - (w * (\vec{A}.\vec{D})) \quad (20)$$

$$\vec{X}(t+1) = (w * \vec{D}'.e^{bl}.cos\,(2\pi l)) + \vec{X}^*(t) \quad (21)$$

$$\vec{X}(t+1) = \overrightarrow{X_{rand}} - (w * (\vec{A}.\vec{D})) \quad (22)$$

where t is the current iteration, $\vec{A}$ is the vector coefficient, $\vec{X}^*$ is tht best whale current vector position, $\vec{X}$ is the vector position, $\vec{D}$ is the displacement whale, and w is the weight.

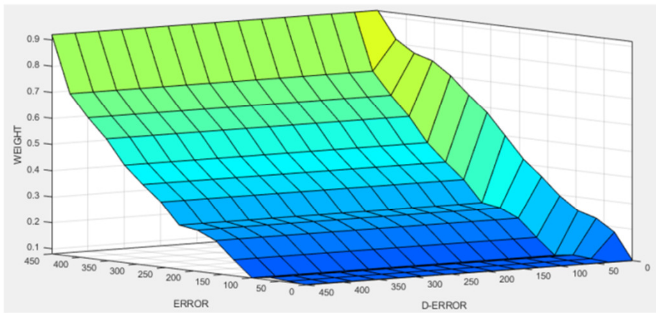

Fig. 5. Surface rules of FLC.

V. DYNAMIC OPTIMAL POWER FLOW

The simulation was conducted using the IEEE 30-bus system data to ensure precise results. To ascertain the highest degree of accuracy, this simulation involved 50 agents and was repeatedly performed 50 times for each test.

A. System Data

This section will describe the system data used in the DOPF simulation employing the WOA and IWOA methods. The dataset, as displayed in Tables I-IV, encompasses the operating cost coefficient, thermal generator capacity, ramp rate, line data, load characteristic, battery parameter, and PV.

TABLE I. PARAMENTER OF THERMAL GENERATOR

Bus No.	Unit	Fuel Cost Function			Pmax (MW)	Pmin (MW)	Ramp Up and Down (MW)
		a ($)	b ($/MWh)	c ($/MWh^2)			
1	1	0	2	0.00375	80	32	±16
2	2	0	1.75	0.0175	80	32	±16
13	3	0	1	0.0625	50	20	±10
22	4	0	3.25	0.00834	55	22	±11
23	5	0	3	0.025	30	12	±6
27	6	0	3	0.025	40	16	±8

TABLE II. LOAD PROFILE FOR 24 HOURS

Hours (am)	**1**	**2**	**3**	**4**	**5**	**6**	**7**	**8**	**9**	**10**	**11**	**12**
Load (MW)	189	184	173	170	173	183	168	171	183	199	201	203
Hours (pm)	1	2	3	4	5	6	7	8	9	10	11	12
Load (MW)	204	206	202	200	205	216	235	261	247	235	212	196

TABLE III. BATTERY PARAMETER

Parameter	**Value (MW)**
Initial Capacity	45
SOC min	15
SOC max	100

TABLE IV. POWER GENERATION IN PHOTO VOLTAGE

Hours	6	7	8	9	10	11	12	13	14	15	16	17	18
MW	0.57	8.13	18.43	27.09	33.04	36.55	37.20	35.12	30.19	23.12	14.33	5.21	0.19

The DOPF optimization was performed using the modified IEEE 30-bus system, as portrayed in Figure 6. This system comprises 30 load buses, six thermal generators connected to buses 1, 2, 13, 22, 23, and 27. The configuration of these generators has been determined by the IEEE system. The relatively distributed location of these generators minimizes losses, which is highly advantageous for this case, as it allows focusing solely on optimizing the generation costs. The system also includes an ES battery at bus 29 and a PV system at bus 30. In the second case, the ES is placed at bus 29, and the PV is placed at bus 30. The inclusion of these two components, a battery and a PV system, increases the complexity of the system. This is due to the fact that both components have generation cost characteristics that differ from those of thermal generators.

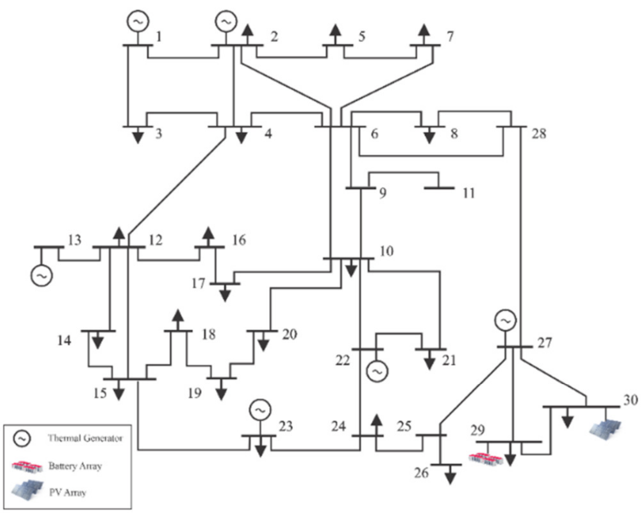

Fig. 6. Modified IEEE 30 bus with PV and battery penetration.

VI. RESULTS AND ANALYSIS

The objective of this simulation is to assess the efficacy of the weights incorporated into the WOA algorithm. The integration of these weights is intended to enhance the performance of the WOA, enabling it to converge more rapidly and accurately toward the global solution. The assessment of the IWOA performance is guided by a set of performance parameters, including the generation cost, computation time, and number of iterations. These criteria are critical for determining the feasibility of implementing the optimization method in real-world electric power systems. Lower generation costs result in reduced operational expenses for utility companies, faster computation times facilitate real-time decision-making, and fewer iterations indicate enhanced computational efficiency. This section presents the outcomes of the DOPF simulations that employ both WOA and IWOA to illustrate the effectiveness of the IWOA. In the initial scenario, designated as the base case, the simulations were conducted exclusively using a thermal generating system. In the subsequent scenario, the simulations incorporated a thermal generation system in conjunction with the PV and battery storage systems. To certify the reliability of the results, ten trials of each method were carried out for each scenario.

A. Base Case

The initial case is considered the base case. This is an IEEE system to be optimized with six thermal generators. In this instance, a comparative analysis is conducted between the WOA and IWOA methods, with the evaluation parameters encompassing the generation cost, computation time, and number of iterations. The simulation results demonstrate that IWOA exhibits superior performance in terms of reduced generation cost and decreased iteration counts when compared to WOA. However, the simulation results indicate that the computation time for both methods is relatively similar. Consequently, the primary advantages of IWOA, namely cost efficiency and iteration reduction, are evident in the simulation results shown in Table V. As depicted in Table V, under the base case scenario, IWOA attains a generation cost of approximately $17 per day and demonstrates a more rapid convergence trajectory in comparison to WOA. The convergence patterns of these two methods are presented in Figure 7. Specifically, IWOA reaches its convergence value by the 19th iteration, whereas WOA requires up to the 25th iteration to achieve convergence.

B. PV and Battery Penetration

In the second case, an analysis is conducted on an IEEE 30-bus system that incorporates six thermal generators, a PV system, and a Battery Energy Storage System (BESS). During daylight hours, the BESS functions as a load, thereby storing excess energy from the PV system and thermal generators. During nocturnal hours, the BESS operates as a generator, hence supplying power to the grid and providing support to the thermal generators during periods of peak demand. A critical factor in this context is the preservation of adequate battery capacity to guarantee a reliable operation during the subsequent days. Analogous to the initial case, a comparative analysis is conducted between the WOA and IWOA methods, employing three criteria: generation cost, computation time, and the number of iterations. The simulation results indicate that IWOA achieves lower generation costs and requires fewer iterations than WOA.

TABLE V. WOA AND IWOA PERFORMANCE

Method	**WOA**		
Number of trials	Time of computation (s)	Number of convergency	Generation cost ($/day)
1	396.24	18	13,401.12
2	392.00	22	13,392.22
3	348.55	25	13,405.91
4	361.63	23	13,393.24
5	348.91	13	13,392.18
6	344.23	18	13,404.65
7	466.14	18	13,405.20
8	413.76	25	13,403.94
9	388.43	20	13,414.10
10	425.74	25	13,395.51
Average	388.57	20.7	13,400.81
Method	IWOA		
Number of trials	Time of computation (s)	Number of convergency	Generation cost ($/day)
1	375.16	18	13,392.52
2	386.96	18	13,386.31
3	384.08	23	13,383.59
4	399.76	25	13,378.53
5	392.57	22	13,377.53
6	402.57	25	13,380.76
7	399.69	19	13,380.84
8	388.69	17	13,383.37
9	390.04	21	13,382.28
10	393.06	17	13,392.20
Average	391.26	20.5	13,383.79

TABLE VI. WOA AND IWOA PERFORMANCE IN PV AND BATTERY PENETRATION

Method	**WOA**		
Number of trials	Time of computation (s)	Number of convergency	Generation cost ($/day)
1	461.15	30	12,755.03
2	457.88	16	12,773.73
3	384.23	25	12,735.89
4	348.89	23	12,763.87
5	503.24	25	12,742.70
6	348.00	14	12,765.37
7	423.74	24	12,743.45
8	351.74	41	12,738.22
9	362.56	20	12,746.54
10	453.00	42	12,749.66
Average	409.44	26	12,751.45
Method	IWOA		
Number of trials	Time of computation (s)	Number of convergency	Generation cost ($/day)
1	409.25	21	12,711.56
2	402.65	15	12,717.18
3	431.10	23	12,727.66
4	470.08	23	12,732.14
5	483.96	19	12,717.66
6	448.86	23	12,726.81
7	444.72	16	12,734.76
8	402.13	23	12,737.02
9	395.35	21	12,727.93
10	407.29	25	12,732.35
Average	429.54	20.9	12,726.51

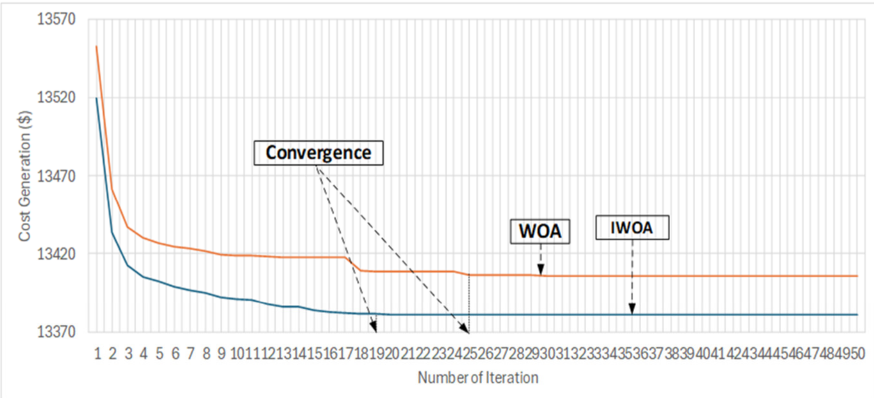

Fig. 7. Convergency curve of the first case.

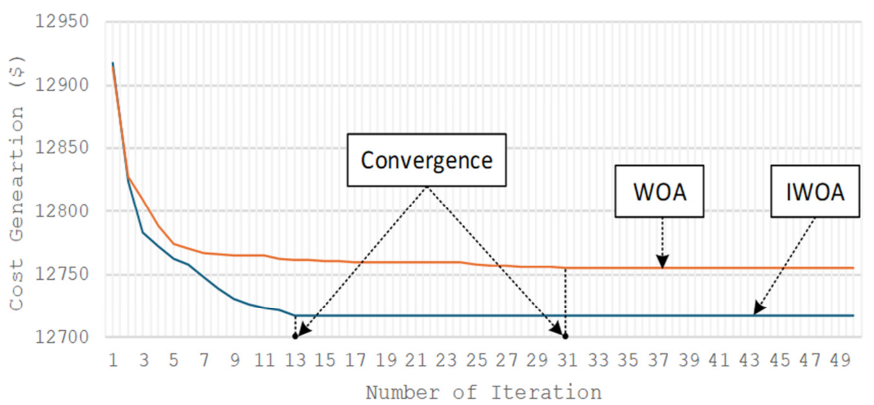

Fig. 8. Convergency curve of the second case.

However, the computation time for both methods is comparable. This finding underscores the notable cost and computational efficiency benefits of IWOA. The comprehensive simulation outcomes are outlined in Table VI.

A comparison of Tables V and VI reveals that the cost of generation in the latter is less expensive than in the former. This is due to the presence of the PV and battery technology, which can supply energy at a negligible cost. From Table VI, it can be observed that in the second case, IWOA achieves a lower generation cost of approximately $25 per day and exhibits faster convergence than WOA. The convergence patterns of these two methods are illustrated in Figure 8. Specifically, IWOA reaches its convergence value by the 13th iteration, whereas WOA requires up to the 31st iteration to achieve convergence.

C. Impact of Photovoltaic and Battery Penetration in Power Generation Profile

The integration of PV and battery ES within the system has been observed to exert a significant influence on the generation profile of the thermal generator. As shown in Figure 9, during daylight hours, 07:00 a.m. – 05:00 p.m., the power generation by the thermal generator exhibits a decline, attributable to the fact that the system is currently receiving augmented power from the PV array. Concurrently, the battery is undergoing charging. Conversely, during nocturnal hours, 6:00 p.m. – 3:00 a.m., the thermal generator's power generation remains lower due to the battery's function as a generator, supplying energy to the system. The battery and PV are both inactive from 4:00 a.m. to 6:00 a.m., with the battery preparing its energy for subsequent operation and the PV awaiting the sunrise.

As demonstrated in Figure 10, the battery's SOC profile was monitored over a 24-hour period. The battery's initial SOC was 45%, and after one day of usage, it returned to that state. This condition is intended to ensure that the battery's availability for subsequent operations remains sufficient.

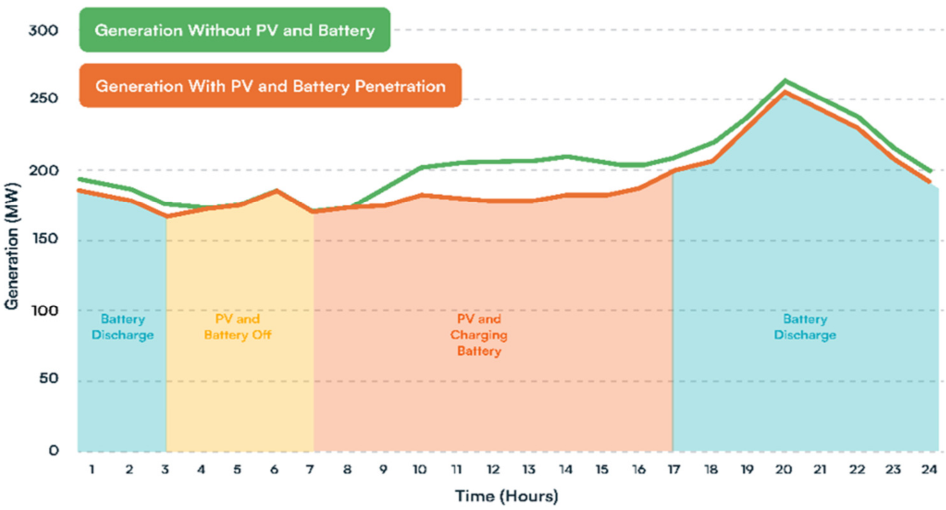

Fig. 9. Curve of power generation by thermal generator.

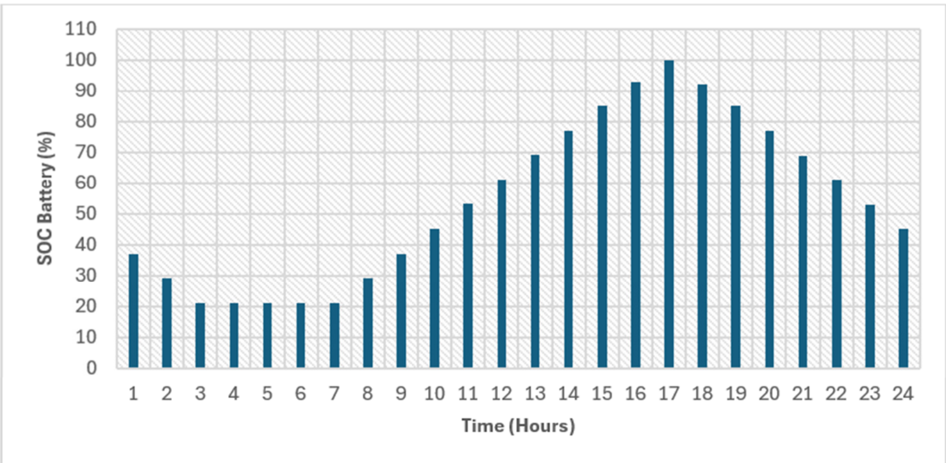

Fig. 10. Battery's SOC profile over a 24-hour period.

D. Statistical analysis

The performance of the proposed method is evaluated through a statistical analysis. A frequently employed technique is the calculation of Standard Deviation (STD). A method with a lower STD is indicative of more stable and superior performance. The calculation of STD is [24]:

$$STDEV.P = \sqrt{\frac{\sum(x-\bar{x})^2}{n}} \tag{23}$$

From cases 1 and 2, data were obtained from 10 trials for each method (WOA and IWOA). The statistical data have been analyzed, yielding the STD values presented in Table VII.

TABLE VII. STD COST GENERTION RESULT

Case	**STD Population**	
	WOA	IWOA
1	6.93	4.90
2	12.01	7.98

The findings indicate that IWOA exhibits superiority over WOA. In the two cases that were examined, IWOA exhibited a lower STD value of 4.9, in comparison to the values of 6.93 and 7.98 observed in cases 1 and 2, respectively. These findings indicate that IWOA can generate more stable power.

VII. CONCLUSIONS

The application of the Whale Optimization Algorithm (WOA) and Improved Whale Optimization Algorithm (IWOA) to the Dynamic Optimal Power Flow (DOPF) problem on the IEEE 30 bus system has yielded promising results. The performance of these two algorithms is evaluated using several performance parameters, including computation time, convergence speed, and optimal value. The performance of these parameters is further validated by the Standard Deviation (STD), thereby ensuring the reliability of the algorithms in producing optimal values. The study yielded several conclusions, including:

- IWOA has demonstrated superiority over WOA in terms of generating more optimal cost values and fewer iterations. The efficacy of IWOA and WOA is substantiated through the implementation of both methods in addressing the DOPF problem on the IEEE 30 bus system. The results indicate that IWOA can achieve generation costs of approximately $17-25/day, which is more economical than the $26/day cost of WOA. Furthermore, IWOA requires approximately 20 iterations, whereas WOA requires 26.
- Furthermore, IWOA has been shown to exhibit a lower STD value in comparison to WOA. This outcome indicates that IWOA exhibits enhanced stability in addressing optimization problems.
- Effective management and planning of Energy Storage (ES) and Photovoltaic (PV) systems can reduce the reliance on thermal power plants and ensure the continuity of the operations the following day.
- The incorporation of a Fuzzy Logic Control (FLC) into the IWOA for generating weights has been demonstrated to enhance its performance, particularly in terms of convergence speed, result accuracy and stability.

ACKNOWLEDGEMENT

The authors are grateful to the Higher Education Financing Center (BPPT), the Endowment Fund for Education Agency (LPDP), and the Indonesian Education Scholarship (BPI) with grant number 202101130735, Directorate of Research and Community Service, Ministry of Education, Culture, Research, and Technology, Institut Teknologi Sepuluh Nopember (ITS) in Surabaya and Politeknik Negeri Madura (Poltera) in Madura, Indonesia for supporting this research.

REFERENCES

[1] H. Bakır, S. Duman, U. Guvenc, and H. T. Kahraman, "A novel optimal power flow model for efficient operation of hybrid power networks," *Computers and Electrical Engineering*, vol. 110, Sep. 2023, Art. no. 108885, https://doi.org/10.1016/j.compeleceng.2023.108885.

[2] I. U. Khan, N. Javaid, K. A. A. Gamage, C. J. Taylor, S. Baig, and X. Ma, "Heuristic Algorithm Based Optimal Power Flow Model Incorporating Stochastic Renewable Energy Sources," *IEEE Access*, vol. 8, pp. 148622–148643, 2020, https://doi.org/10.1109/ACCESS.2020.3015473.

[3] M. Wang, H. B. Gooi, S. Chen, and S. Lu, "A mixed integer quadratic programming for dynamic economic dispatch with valve point effect," in *2015 IEEE Power & Energy Society General Meeting*, Denver, CO, USA, Jul. 2015, pp. 1–10, https://doi.org/10.1109/PESGM.2015.7285846.

[4] T. A. A. Victoire and A. E. Jeyakumar, "Reserve constrained dynamic dispatch of units with valve-point effects," *IEEE Transactions on Power Systems*, vol. 20, no. 3, pp. 1273–1282, Aug. 2005, https://doi.org/10.1109/TPWRS.2005.851958.

[5] A. A. Mohamed and B. Venkatesh, "Line-Wise Optimal Power Flow Using Successive Linear Optimization Technique," *IEEE Transactions on Power Systems*, vol. 34, no. 3, pp. 2083–2092, May 2019, https://doi.org/10.1109/TPWRS.2018.2881254.

[6] R. S. Ferreira, C. L. T. Borges, and M. V. F. Pereira, "A Flexible Mixed-Integer Linear Programming Approach to the AC Optimal Power Flow in Distribution Systems," *IEEE Transactions on Power Systems*, vol. 29, no. 5, pp. 2447–2459, Sep. 2014, https://doi.org/10.1109/TPWRS.2014.2304539.

[7] Y. Xia and K. W. Chan, "Dynamic constrained optimal power flow using semi-infinite programming," *IEEE Transactions on Power Systems*, vol. 21, no. 3, pp. 1455–1457, Aug. 2006, https://doi.org/10.1109/TPWRS.2006.879241.

[8] J. C. López, P. P. Vergara, C. Lyra, M. J. Rider, and L. C. P. da Silva, "Optimal Operation of Radial Distribution Systems Using Extended Dynamic Programming," *IEEE Transactions on Power Systems*, vol. 33, no. 2, pp. 1352–1363, Mar. 2018, https://doi.org/10.1109/TPWRS.2017.2722399.

[9] S. E. Kayacık and B. Kocuk, "An MISOCP-Based Solution Approach to the Reactive Optimal Power Flow Problem," *IEEE Transactions on Power Systems*, vol. 36, no. 1, pp. 529–532, Jan. 2021, https://doi.org/10.1109/TPWRS.2020.3036235.

[10] M. A. M. Shaheen, H. M. Hasanien, S. F. Mekhamer, and H. E. A. Talaat, "Optimal Power Flow of Power Systems Including Distributed Generation Units Using Sunflower Optimization Algorithm," *IEEE Access*, vol. 7, pp. 109289–109300, 2019, https://doi.org/10.1109/ACCESS.2019.2933489.

[11] A. Baziar, R. Bo, M. D. Ghotbabadi, M. Veisi, and W. Ur Rehman, "Evolutionary Algorithm-Based Adaptive Robust Optimization for AC Security Constrained Unit Commitment Considering Renewable Energy Sources and Shunt FACTS Devices," *IEEE Access*, vol. 9, pp. 123575–123587, 2021, https://doi.org/10.1109/ACCESS.2021.3108763.

[12] M. A. Ilyas, G. Abbas, T. Alquthami, M. Awais, and M. B. Rasheed, "Multi-Objective Optimal Power Flow With Integration of Renewable

Energy Sources Using Fuzzy Membership Function," *IEEE Access*, vol. 8, pp. 143185–143200, 2020, https://doi.org/10.1109/ACCESS.2020.3014046.

[13] M. R. AlRashidi and M. E. El-Hawary, "Hybrid Particle Swarm Optimization Approach for Solving the Discrete OPF Problem Considering the Valve Loading Effects," *IEEE Transactions on Power Systems*, vol. 22, no. 4, pp. 2030–2038, Nov. 2007, https://doi.org/10.1109/TPWRS.2007.907375.

[14] K. Widarsono, F. D. Murdianto, M. Nur, and A. Mustofa, "Optimal power flow using particle swarm optimization for IEEE 30 bus," *Journal of Physics: Conference Series*, vol. 1595, no. 1, Jul. 2020, Art. no. 012033, https://doi.org/10.1088/1742-6596/1595/1/012033.

[15] R. Jamal, B. Men, and N. H. Khan, "A Novel Nature Inspired Meta-Heuristic Optimization Approach of GWO Optimizer for Optimal Reactive Power Dispatch Problems," *IEEE Access*, vol. 8, pp. 202596–202610, 2020, https://doi.org/10.1109/ACCESS.2020.3031640.

[16] K. Widarsono, A. Soeprijanto, and R. S. Wibowo, "Dynamic Optimal Power Flow Considering Valve Point Effect And Energy Storage Utilization Using Whale Optimization Algorithm," in *2022 14th International Conference on Information Technology and Electrical Engineering (ICITEE)*, Yogyakarta, Indonesia, Oct. 2022, pp. 189–194, https://doi.org/10.1109/ICITEE56407.2022.9954109.

[17] J. Fang, Q. Zeng, X. Ai, Z. Chen, and J. Wen, "Dynamic Optimal Energy Flow in the Integrated Natural Gas and Electrical Power Systems," *IEEE Transactions on Sustainable Energy*, vol. 9, no. 1, pp. 188–198, Jan. 2018, https://doi.org/10.1109/TSTE.2017.2717600.

[18] M. S. Nazir, Z. M. Ali, M. Bilal, H. M. Sohail, and H. M. N. Iqbal, "Environmental impacts and risk factors of renewable energy paradigm-a review," *Environmental Science and Pollution Research International*, vol. 27, no. 27, pp. 33516–33526, Sep. 2020, https://doi.org/10.1007/s11356-020-09751-8.

[19] A. S. Al-Ezzi and M. N. M. Ansari, "Photovoltaic Solar Cells: A Review," *Applied System Innovation*, vol. 5, no. 4, Aug. 2022, Art. no. 67, https://doi.org/10.3390/asi5040067.

[20] S. Mirjalili and A. Lewis, "The Whale Optimization Algorithm," *Advances in Engineering Software*, vol. 95, pp. 51–67, May 2016, https://doi.org/10.1016/j.advengsoft.2016.01.008.

[21] I.-M. Chao, S.-C. Hsiung, and J.-L. Liu, "Improved Whale Optimization Algorithm Based on Inertia Weights for Solving Global Optimization Problems," *Advances in Technology Innovation*, vol. 5, no. 3, pp. 147–155, Jul. 2020, https://doi.org/10.46604/aiti.2020.4167.

[22] G. Ma and X. Yue, "An improved whale optimization algorithm based on multilevel threshold image segmentation using the Otsu method," *Engineering Applications of Artificial Intelligence*, vol. 113, Aug. 2022, Art. no. 104960, https://doi.org/10.1016/j.engappai.2022.104960.

[23] J. Zhang and J. S. Wang, "Improved Whale Optimization Algorithm Based on Nonlinear Adaptive Weight and Golden Sine Operator," *IEEE Access*, vol. 8, pp. 77013–77048, 2020, https://doi.org/10.1109/ACCESS.2020.2989445.

[24] K. Widarsono, A. Soeprijanto, R. S. Wibowo, N. K. Aryani, B. Oktaviani, and M. Nur, "Dynamic Optimal Power Flow with PV and BMS Integration in the Power Grid Using TFWO Method," in *International Conference on Artificial Intelligence and Mechatronics System, AIMS 2024*, Indonesia, 2024, https://doi.org/10.1109/AIMS61812.2024.10512713.